NeuroImage 49 (2010) 1066–1072

Contents lists available at ScienceDirect

NeuroImage

journal homepage: www.elsevier.com/locate/ynimg

Neurofeedback: A promising tool for the self-regulation of emotion networks

S.J. Johnston [a], S.G. Boehm [a], D. Healy [b,c], R. Goebel [d], D.E.J. Linden [a,c,*]

[a] Bangor Imaging Unit, Wolfson Centre for Clinical and Cognitive Neuroscience, School of Psychology, Bangor University, Bangor, UK
[b] Department of Psychological Medicine, Cardiff University, Cardiff, UK
[c] North West Wales NHS Trust, Bangor, UK
[d] Department of Cognitive Neuroscience, Faculty of Psychology and Neuroscience, Maastricht University, Maastricht, Netherlands

ARTICLE INFO

Article history:
Received 26 March 2009
Revised 3 July 2009
Accepted 22 July 2009
Available online 29 July 2009

Keywords:
Emotion
Neurofeedback
Functional magnetic resonance imaging
Insula
Amygdala
Striatum

ABSTRACT

Real-time functional magnetic resonance imaging (fMRI) affords the opportunity to explore the feasibility of self-regulation of functional brain networks through neurofeedback. We localised emotion networks individually in thirteen participants using fMRI and trained them to upregulate target areas, including the insula and amygdala. Participants achieved a high degree of control of these networks after a brief training period. We observed activation increases during periods of upregulation of emotion networks in the precuneus and medial prefrontal cortex and, with increasing training success, in the ventral striatum. These findings demonstrate the feasibility of fMRI-based neurofeedback of emotion networks and suggest a possible development into a therapeutic tool.

Introduction

Psychological interventions for mental disorders are commonly validated for their clinical rather than their biological effects. However, it is increasingly recognised that a better understanding of the neural changes accompanying successful psychotherapy may have considerable benefits. For example, if we are able to identify pathological activation patterns in relation to psychiatric symptoms, and if these patterns normalise after intervention, we may use this information in the development of new treatment protocols targeting the functional correlates of specific brain networks. To take the matter one step further, we might even be able to target these pathological networks directly, through neurofeedback (Linden, 2006). Several decades of feedback research with EEG signals have shown that participants can be trained to influence the amplitude or topography of specific components of scalp electric activity (Birbaumer et al., 2006). However, it has been very difficult to influence specific mental states or treat psychiatric disorders with EEG-based neurofeedback, probably because of its low spatial specificity and difficulties associated with the poor signal to noise ratio provided by single trial based EEG.

The development of fMRI (functional magnetic resonance imaging)-based neurofeedback (Weiskopf et al., 2004b; deCharms, 2007) has enabled the regulation of brain activity with much higher spatial precision. Participants are trained to influence the fMRI signal from a target area while they receive online information about the amplitude of this signal. There is a delay of ca. 6 s between neural activity and the feedback signal, resulting from the haemodynamic lag. Given the success of fMRI-neurofeedback, it is fair to assume that participants can accommodate this delay. Target areas are selected on the basis of anatomical (e.g., anterior cingulate [Weiskopf et al., 2003]; anterior insula [Caria et al., 2007]; inferior frontal gyrus [Rota et al., 2009]) or functional (e.g., presentation of faces and houses [Weiskopf et al., 2004a]) criteria. Optimal training effects seem to be achieved when participants find an internal active task that reliably activates the respective region(s).

In the present work we used fMRI to identify areas reactive to positive and negative emotional stimuli, and then fMRI-neurofeedback to train participants to upregulate the target areas associated with processing negative stimuli. We show that brain networks associated with specific emotions can indeed be regulated by means of neurofeedback.

Materials and methods

Participants

Thirteen volunteers (4 males, 9 females, age range 21–52) participated in the experiment after giving informed consent. The experimental protocol was approved by the ethics committees of the School of Psychology, Bangor University, and the North West Wales NHS Trust. Participants had no history of neurological or psychiatric

* Corresponding author. School of Psychology, Bangor University, Bangor LL57 2AS, UK. Fax: +44 1248382500.
E-mail address: d.linden@bangor.ac.uk (D.E.J. Linden).

1053-8119/$ – see front matter © 2009 Elsevier Inc. All rights reserved.
doi:10.1016/j.neuroimage.2009.07.056

illness. All participants were debriefed after the experiment and were interviewed about any distress experienced as a consequence of the procedure, which they all denied.

Psychometric testing

In order to document changes in mood state with a more fine-grained measure than a debriefing interview, we administered the Profile of Mood States (POMS, Lorr et al., 1971) and Positive and Negative Affect Scale (PANAS, Watson et al., 1988) to five of the participants immediately before and after the neurofeedback session. The PANAS assesses current positive and negative affect by asking participants to rate themselves in relation to ten positive (e.g., "attentive") and negative (e.g., "hostile") terms on a 5-point Likert scale. The POMS is based on self-ratings along the six dimensions Tension-anxiety, Anger-hostility, Fatigue-inertia, Depression-dejection, Vigor-activity, and Confusion-bewilderment. It allows for the computation of a "total mood disturbance" (TMD), which will be reported here. Because of the preliminary character of the psychometric assessments, results will only be reported descriptively.

fMRI localiser

We used pictures with negative (mean normative ratings for valence 2.8 [SD .42], arousal 5.63 [SD .55]), positive (valence 6.90 [.55], arousal 6.00 [.74]) and neutral valence (valence 5.45 [.56], arousal 3.44 [.47]) (see Suppl. Figs. 1a–c) from the International Affective Pictures System (IAPS) (Lang et al., 1999) to identify emotion-responsive areas with fMRI on a 3 Tesla Philips Achieva system (TR = 2 s, TE = 30 ms, 30 slices, 3 mm slice thickness, inplane resolution 2 mm × 2 mm). IAPS pictures have been pre-tested in normative samples for their valence (probing the emotion evoked in the participants with a scale from 1 to 9, ranging from "unhappy" to "happy") and arousal (scale from 1 to 9, ranging from "calm" to "excited"). We presented four pictures of the same emotion category in blocks of 6 s (1.5 s per picture), alternating with a fixation baseline of 12 s. We presented 12 blocks per category in a pseudorandom order. We computed an online general linear model on these raw data with three predictors corresponding to the three picture categories, convolved with a haemodynamic reference function, using the Turbo-BrainVoyager software package (Brain Innovation B. V., Maastricht, the Netherlands). This enabled us to obtain and localise the emotion networks of individual participants, and select an individually tailored, maximally responsive, target area. We hypothesised that this approach would lead to much reduced learning times compared to anatomically defined target areas.

We used the brain area with the highest response to negative compared to neutral pictures as the target area, identified online on the original 2-dimensional data. For further analysis across individuals, we converted these regions of interest into Talairach space (Table 1). Target areas were in the ventrolateral prefrontal cortex (VLPFC)/insula or the medial temporal lobe (MTL)/amygdala, unilaterally or bilaterally.

Neurofeedback

The participants were instructed to upregulate their target region activity for periods of 20 s ("up"), alternating with baseline periods of 14 s ("rest") (12 up-rest cycles per run). Thus, one training run lasted for 408 s. Four participants underwent two, and nine participants three neurofeedback runs, yielding an overall training time per participant between ca. 14 and 21 min. All runs were conducted in a single session in the scanner. Imaging parameters were as described above.

We suggested that emotional imagery might be employed but did not prescribe a specific strategy, suggesting instead that participants should monitor the feedback signal and 'tune' their strategy during successive blocks to determine the most efficient approach. In this respect our instructions were different from those used by Posse et al. (2003), who employed a mood induction paradigm with additional feedback on amygdala activity. For the continuous feedback provided in our study, we used the picture of a thermometer whose temperature reflected amplitude increases of the fMRI signal in the target area, relative to a baseline period (Suppl. Fig. 1d). The thermometer was updated every 2 s to inform participants about their performance.

Table 1
Individual target areas.

Subject no.	Anatomical area	Talairach coordinates: $x/y/z$	No. of voxels
1	Bilateral amygdala	RH: 19/−2/−9; LH: −24/−2/−8	3210
2	Left VLPFC	−50/18/11	128
3	Right insula	27/20/13	838
4	Right amygdala/MTL	24/−10/−16	2418
5	Right insula	30/19/−4	328
6	Bilateral VLPFC/insula	RH: 43/16/−4; LH: −40/15/2	7885
7	Right VLPFC/insula	44/18/1	3513
8	Right insula	34/10/−2	981
9	Right VLPFC	38/33/7	3531
10	Bilateral VLPFC/insula	RH: 41/12/5; LH: −24/11/3	8186
11	Bilateral VLPFC/insula	RH: 43/9/12; LH: −37/12/8	5520
12	Right VLPFC	56/25/4	740
13	Left VLPFC/insula	−43/5/2	1411

Data analysis

Online ('real time') fMRI was made possible via a fast connection between the MRI scanner and the analysis/display computer. After acquisition and reconstruction, data from the scanner is sent to the analysis computer. The real time fMRI software, Turbo-BrainVoyager detected, imported and analysed the data, corrected them for angular and translational motion in the Cartesian coordinate system and added them to an incremental general linear model calculation. The resultant signal estimate for each incoming functional imaging volume within the selected region-of-interest was 'fed back' to the participant using the in-built 'thermometer' display. Delay time between the image collection and presentation of the feedback signal to the participant was less than 100 ms.

Offline, the raw data was further pre-processed using the BrainVoyager software package. In order to remove artefacts resulting from factors such as physiological noise and long-term drift; the additional offline postprocessing procedures include linear trend removal and temporal high pass filtering (low cutoff: 3 cycles per run). To enable analysis across participants, we normalised anatomical and functional data into the Talairach coordinate system (with new cubic voxel dimensions of 2 mm edge length) and spatially smoothed the functional data with a 4 mm full width at half maximum Gaussian kernel. For the localiser runs, we computed a random-effects general linear model (GLM) with three predictors for the negative, positive and neutral pictures, convolved with a haemodynamic reference function, and the six motion confounds. For the neurofeedback runs, we computed a random-effects GLM with one predictor for the regulation state (up, rest), convolved with a haemodynamic reference function, and the six motion confounds.

Region-of-interest analysis

We computed region-of-interest (ROI) GLM's for each of the neurofeedback runs across the target areas identified by the localiser run (Table 1) and extracted the beta values for the "up" vs. "rest" periods for each participant. This allowed us statistically to compare the activation levels in the individual target areas during

neurofeedback vs. baseline and during late vs. early neurofeedback runs in a group analysis.

Whole-brain analysis

We performed whole-brain analyses for the localiser runs and computed contrasts for conditions vs. baseline (for the negative, positive and neutral predictors) and between conditions. The effects vs. baseline were thresholded at $p<.01$. Correction for multiple comparison was achieved by cluster-level thresholding using the Monte Carlo simulation tool implemented in BrainVoyager (>288 mm^3). The three maps were superimposed on coronal slices of one participant's brain to yield an overlay map (Fig. 1). We also computed the contrast negative vs. positive (using the same threshold) (Fig. 2, Table 2). For the 20 neurofeedback runs, we similarly computed a GLM and analysed effects ("up" vs. rest) and contrasts between predictors (the "up" predictor for the first vs. the last runs). Because our aim was to illustrate the most salient whole-brain effects of neurofeedback, we applied a conservative threshold of $p<.001$ (cluster-level threshold: 250 mm^3). For the contrast "early" vs. "late" we applied the threshold $p<.05$ (false discovery rate, FDR, fixed-effects analysis), cluster size >500. All suprathreshold clusters for the neurofeedback analysis are documented in Tables 3 and 4. For selected regions, we computed event-related average time courses (computing the percent change of the fMRI blood oxygenation dependent [BOLD] signal against a baseline comprising the three time points before each "up" period) for the activation across all neurofeedback runs (Fig. 4) and separately for early and late runs (Fig. 5).

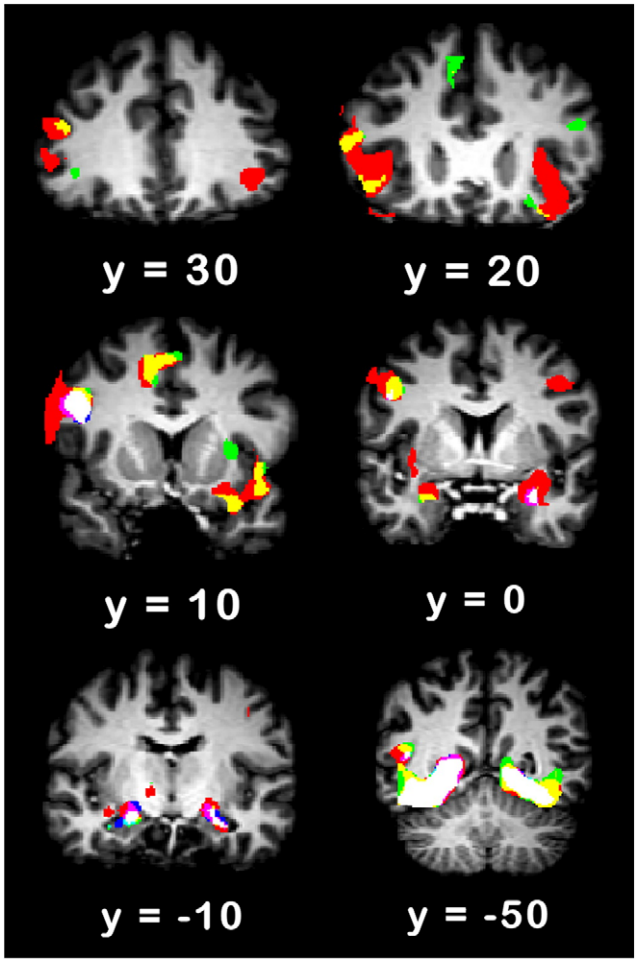

Fig. 1. Emotion networks. Five coronal slices show overlap maps with the areas responsive to negative (red), positive (green) and neutral (blue) emotions, thresholded at $p<.01$, cluster size >288 mm^3. If more than one area was active, colour additions were computed by the Red-Green-Blue (RGB) system. For example, yellow areas would denote the overlap between positive (green) and negative (red) emotions.

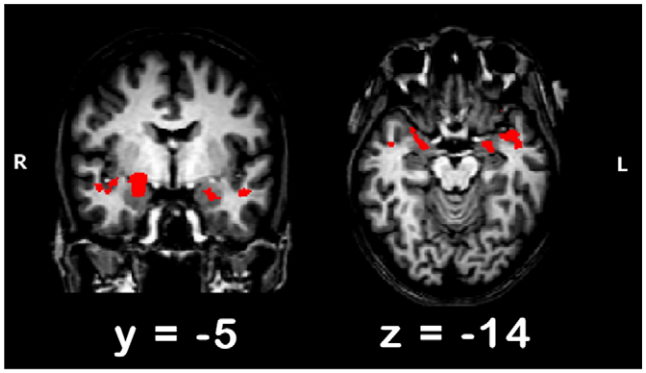

Fig. 2. Negative vs. positive emotions. The contrast between activity to negative and positive pictures, thresholded at $p<.01$, cluster size >288 mm^3; areas in red denote significantly more activation to negative vs. positive pictures. The left panel shows activity in the bilateral VLPFC and amygdalae (sagittal slice at Talairach $y=-5$), the right panel activity in bilateral amygdala (transverse slice at Talairach $z=-14$).

Results

First we localised areas responsive to pictures with negative emotional content with a localiser task online during the scanning session. These areas were located in the VLPFC/insula region or in the MTL, including the amygdala, in all participants (Table 1). The whole-brain GLM of the localiser experiment revealed widespread activation for all picture categories in prefrontal and medial temporal regions (Fig. 1), and in occipitotemporal and parietal higher visual areas. The overlay maps of Fig. 1 indicate that the activation was most extensive for the negative pictures, particularly in the MTL, insula and VLPFC. Statistical contrasts between negative and positive pictures yielded higher activation for negative pictures in the bilateral VLPFC/insula region, and extended amygdala, dorsomedial prefrontal cortex (DMPFC), right premotor cortex (PMC) and left superior temporal sulcus (STS) (Fig. 2, Table 2).

In the neurofeedback runs, participants were instructed to upregulate activation in their individually defined target areas (for an example see Fig. 3a). All participants were able to produce higher activation of the target area during "up" compared to "rest" periods (Fig. 3c). The ROI-GLM revealed that these changes were significant at the group level already during the first run ($t(12)=3.98$, $p=.002$, two-tailed).

All participants used negative imagery or memories. Reported strategies included imagery of terrifying scenes, imagery of themselves in distressing situations, sad memories, and thinking about

Table 2
Areas with significantly higher activity for negative vs. positive emotions in the localiser run.

Anatomical name	Talairach coordinates: $x/y/z$	No. of voxels
Right hemisphere		
VLPFC/insula	41/24/8	1937
PMC	50/3/40	539
Extended amygdala	26/−4/−8	2196
Left hemisphere		
Anterior insula	−32/20/−4	424
Posterior insula	−37/3/−10	1000
Amygdala	−22/−4/−13	305
STS	−44/−57/16	477
Across midline		
DMPFC	5/54/29	1556

Activation clusters for the contrast between the localiser predictors for the positive vs. negative picture conditions. Random-effects analysis thresholded at $p<.01$, cluster size >288 mm^3.

Table 3
Areas activated during neurofeedback.

Anatomical name	Talairach coordinates: $x/y/z$	No. of voxels
Right hemisphere		
Extended amygdala	19/−9/−2	391
Left hemisphere		
Ventromedial thalamus	−7/−13/10	325
Dorsal striatum	−22/4/11	272
DMPFC	−8/49/38	426
VLPFC/insula	−42/17/11	559
Basal forebrain/S. innominata	−21/3/−5	696
Cuneus/PCC	−8/−48/11	1477
Bilateral across midline		
ACC	0/14/24	272

Activation clusters for the neurofeedback predictor for all runs. Random effects analysis thresholded at $p<.001$, cluster size >250 mm^3.

people they disliked. All participants reported trying several strategies until they settled for the one that worked best (that is, giving them optimum control over the thermometer), normally in the final run. Activation levels increased further during subsequent training runs in eleven of the participants (Fig. 3c) (significant training-related increase at group level: $t(12)=2.47$, $p<.029$, two-tailed).

We investigated whether any areas would support this type of neurofeedback across participants beyond the specific individual target area with the whole-brain GLM. This analysis revealed that activation increases during the upregulation periods were not confined to the target areas (such as left insula and right amygdala), but included areas in the left DMPFC, striatum and basal forebrain, parietal cortex (precuneus) and posterior cingulate, and the anterior cingulate (ACC) bilaterally (Fig. 4, Table 3).

We investigated the neural basis for the additional learning effect comparing the levels of activation during the last (and most efficient) neurofeedback run to the first. This comparison revealed a robust signal increase in the right ventral striatum as well as in bilateral prefrontal areas and insula and postcentral gyrus (Fig. 5, Table 4). The random-effects contrast for the training-related increase in the right ventral striatum was also significant ($t(12)=2.76$, $p=.017$, two-tailed).

The average scores on the PANAS changed from 26.8 to 20.2 (positive) and 10.8 to 12.2. (negative) after pre- vs. post-neurofeedback. The average TMD on the POMS increased from −4.6 to 12.4, with four out of the five participants who underwent psychometric testing showing higher mood disturbance after the neurofeedback session. However these, as all the other participants, did not report distress or any relevant effect on their wellbeing at debriefing.

Discussion

The rapid training success (reliable upregulation of the target area already during the first run in most participants) conforms to previous reports of training success for motor cortex (deCharms et al., 2004) and anterior cingulate (deCharms et al., 2005).

Common strategies documented in previous neurofeedback work included motor imagery (deCharms et al., 2004) and modulation of attention (deCharms et al., 2005; Yoo et al., 2006). It is noteworthy that in the present study training success was similar for areas

Table 4
Areas with increased activation in the last vs. first feedback runs.

Anatomical name	Talairach coordinates: $x/y/z$	No. of voxels
Right hemisphere		
Ventral striatum	9/5/6	712
VLPFC/insula	32/7/5	3832
DMPFC	13/30/37	903
Postcentral gyrus	45/−28/42	1214
Left hemisphere		
DLPFC	−22/10/35	1353
DMPFC	−16/41/30	587
VPMC	−47/−7/34	927
Insula	−23/12/17	857
Postcentral gyrus	−40/−26/40	1103

Activation clusters for the contrast between the neurofeedback predictors for the last vs. first runs of each participant. Fixed effects analysis thresholded at FDR $p<.05$, cluster size >500.

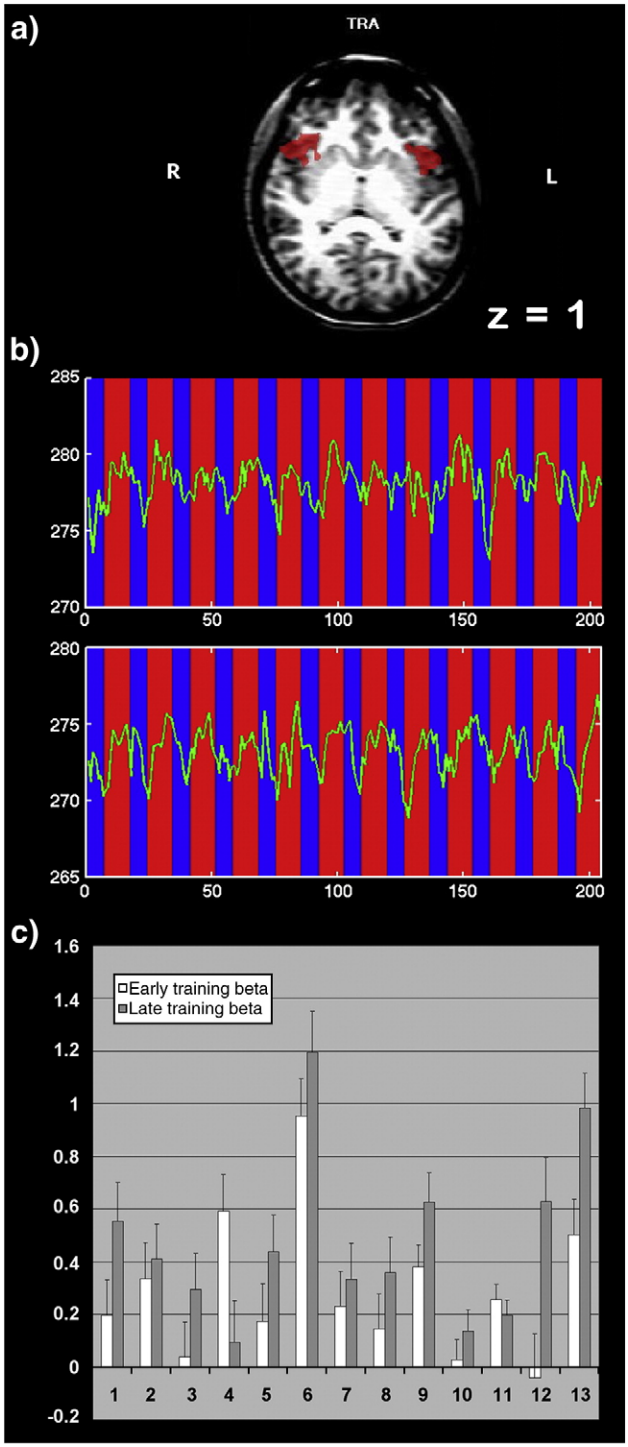

Fig. 3. Neurofeedback training effects. a) Example of a target area for the neurofeedback protocol (participant 6: bilateral insula). b) The mean time course for this area during the first and last neurofeedback runs of this participant (from top to bottom). "Up" periods are coloured in red, "rest" periods in blue. c) Beta estimates for the upregulation during early and late training for the thirteen individual participants. The panel shows that all but one participant achieved self-control during the first training run, and that likewise all but two achieved further increase towards the late training.

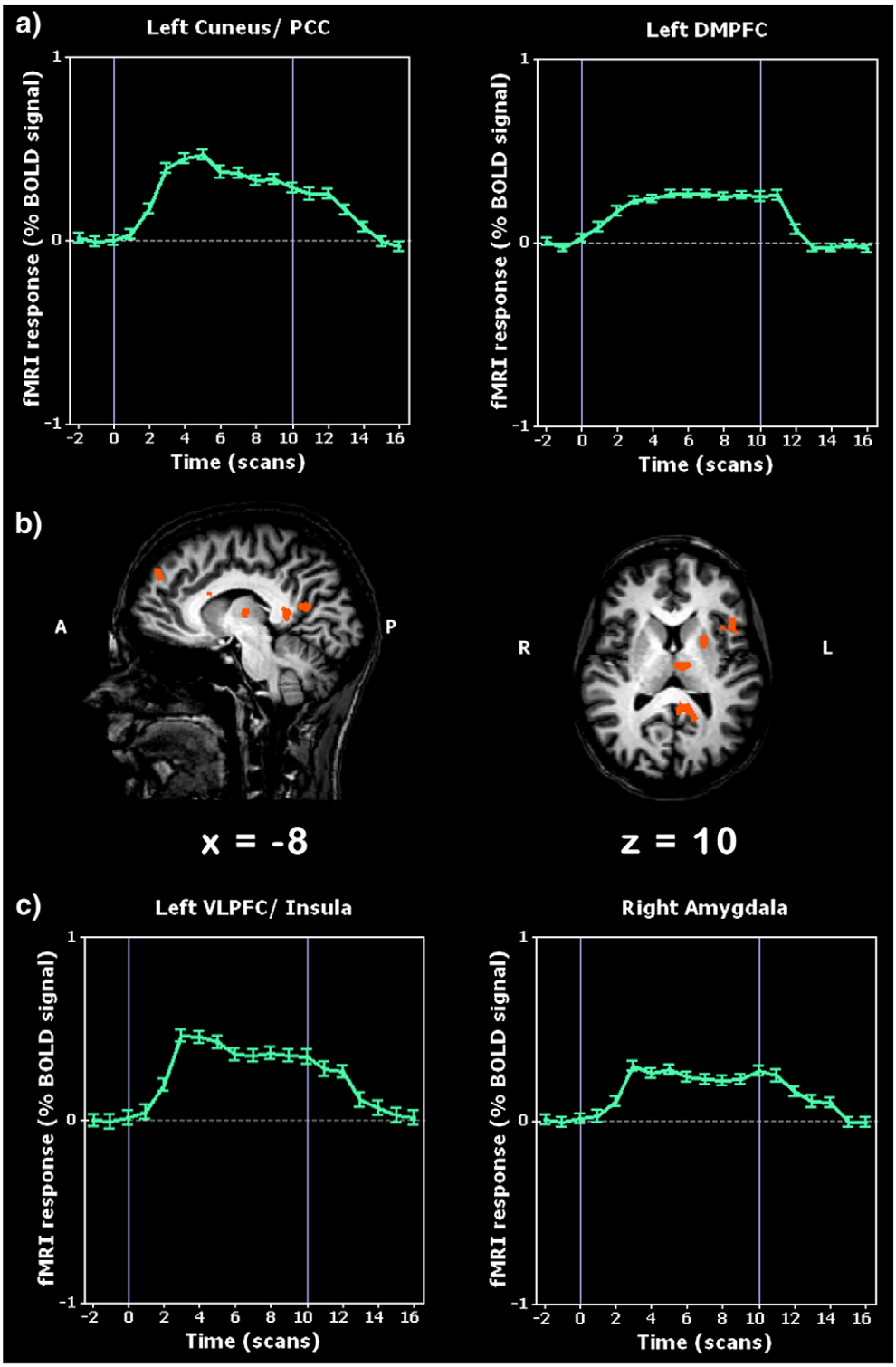

Fig. 4. A neurofeedback network. The clusters of highest activation during upregulation periods across participants in dorsomedial prefrontal cortex, left insula and precuneus (central pane) with their average time courses. The vertical bars denote the duration of the "up" period. The horizontal slice also shows activity in the bilateral ventral striatum. The map is thresholded at $p<.001$ (cluster size >250 mm^3).

associated with a specific emotion. This approach is different from traditional imagery or mood induction experiments, where the experimenter prescribes a strategy and then searches for associated brain areas (e.g. Harrison et al., 2008). Here we prescribed a brain area, and participants had to search for the appropriate strategy to activate it. From the subjective accounts it became clear that imagery of the previously viewed affective scenes, from the localiser task, was not the most effective strategy, and all participants finally settled for a strategy that involved personal memories. This use of a flexible strategy extends the pioneering work of deCharms et al. (2005) where a successful training effect in anterior cingulate was obtained through the participants following prescribed imagery approaches. The aim of the deCharms et al. (2005) study was to determine the effect of successful auto-regulation of rostral anterior cingulate cortex (rACC),

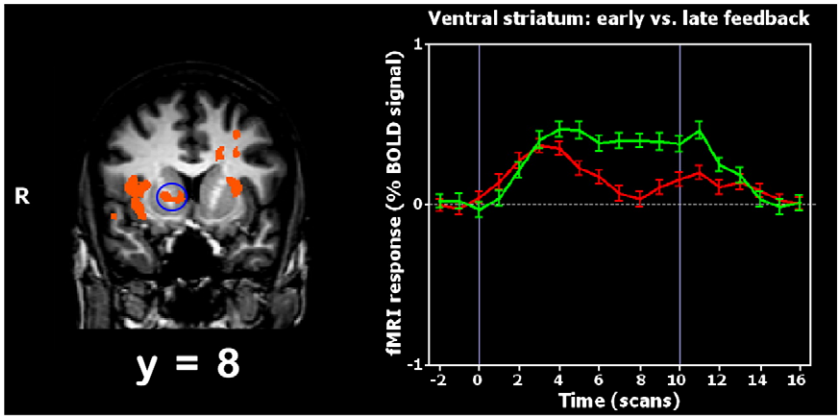

Fig. 5. Training-related activation. Contrast map for the upregulation predictor during the last vs. the first runs for each participant, showing activation increases in the right ventral striatum and insula (left). The averaged time courses in the right ventral striatum are shown for the first (red) and last (green) neurofeedback run (right). Thresholded at FDR $p<.05$, cluster size >500 mm^3.

known to be involved in pain processing, on participants' ratings of pain to a noxious thermal stimulus. Prescribed imagery may be less effective when participants need to generate a specific emotion in order to upregulate a brain area, and where a participant's specific response is key to successful regulation as opposed to the 'physical' properties of the negative stimulus itself (Roseman et al., 1990). Our participants all reported using imagery and memories pertaining to their own personal past, but there were considerable inter-individual differences in the actual strategies and content used.

The localiser procedure identified a network of brain areas that is commonly found active in response to emotional stimuli. The strongest activation was observed for negative pictures, with activity in the bilateral amygdalae, VLPFC and insula particularly prominent. Amygdala activation has often been associated with fear, and insula with disgust. Thus, this activation pattern matches the content of the negative IAPS pictures, many of which display violent scenes or disgusting material. Future studies may seek to confine the localiser for negative emotions to just one of the primary emotions in order to improve selectivity.

Although we did not perform subjective ratings of the emotions induced by our localiser procedure, we are confident that we were successful in transiently inducing the appropriate negative and positive mood states. First, we used pictures that had received relatively high arousal ratings from normative samples for both the negative and the positive condition. Second, the networks activated by both emotional categories largely corresponded to those identified with the respective mood induction procedures (Phan et al., 2002; Harrison et al., 2008).

The activation of the additional areas that were reliably activated across participants, outside of those used as the individual target areas and areas of the extended limbic system, which would be expected to be involved in emotional imagery and memories, may allow inferences about the neural and psychological mechanisms supporting the training success. Precuneus activation has been reported in the absence of visual stimulation when participants engaged in visual imagery (Cavanna and Trimble, 2006) and has also been implicated in self-awareness and self-monitoring (Cojan et al., 2009). Similarly, activity in somatosensory cortex (postcentral gyrus) may be related to heightened self-awareness during the training process.

Both posterior cingulate and retrosplenial cortex are specifically involved in retrieving autobiographical memories, compared to imagined events (Summerfield et al., 2009), which would conform to our participant's preferred strategy of evoking autobiographical memories of sad or otherwise distressing events. The activation of the ventral striatum in relation to training progress may indicate intrinsic reward-like properties of the learning success (Carelli, 2002; Day and Carelli, 2007; Talmi et al., 2008).

The whole-brain effects of fMRI-neurofeedback have been investigated in a previous study, which used the anatomically defined right anterior insula as the target area (Caria et al., 2007), rather than using a functional and participant-specific localiser. This study did not find any significant activation increase across training runs outside the target areas. In the present study, the self-regulation was not a purely local effect but, regardless of individual target areas, involved medial prefrontal areas associated with self-referential processing, lateral prefrontal areas associated with cognitive control, striatal systems implicated in reward-based learning and retrosplenial areas associated with mental imagery and self-awareness. The choice of target area through a functional rather than anatomical localiser may have resulted in a higher salience for the participants and thus contributed to this pattern of training-related activation. One limitation of our study is that it did not control for non-specific training effects. However, previous studies have already demonstrated that when participants receive sham feedback or engage in mental imagery alone, they do not show similar training effects (Caria et al., 2007; deCharms et al., 2004, 2005). It is also interesting to note that cognitive effort alone is unlikely to have resulted in increased activity in the target areas because a recent study has shown reduced rather than increased response of the right insula and bilateral amygdalae to negative pictures during a concurrent demanding cognitive task (Van Dillen et al., 2009).

The subset of participants who underwent psychometric testing showed increased mood disturbance, mainly based on increasing self-ratings of negative affect. This suggests that the neurofeedback procedure had an effect on the participants' mood, although we cannot distinguish between effects of the self-regulation itself and the strategies participants used to achieve it. These effects might be dissociated by protocols employing sham neurofeedback. Future studies may also usefully employ measures of emotion that are not based on self-report, such as skin conductance or heart rate. Finally, a crucial question for any clinical application remains whether similar effects can be obtained for positive mood induction, either by upregulation of positive or downregulation of negative emotion networks. Because of the high degree of overlap between the networks that respond to stimuli with positive and negative valence, more spatially selective approaches may be needed. Ultimately the aim for clinical applications of emotion-related neurofeedback would be to equip participants or patients with strategies to help them achieve desired mental states that they can also practice outside the MRI laboratory.

Acknowledgments

This research was supported by the Wales Institute of Cognitive Neuroscience (WICN) and the North West Wales NHS Trust. SGB is a Research Councils UK (RCUK) fellow. We are grateful to Sian Lowri Griffiths for the help with data analysis.

Appendix A. Supplementary data

Supplementary data associated with this article can be found, in the online version, at doi:10.1016/j.neuroimage.2009.07.056.

References

Birbaumer, N., Weber, C., Neuper, C., Buch, E., Haapen, K., Cohen, L., 2006. Physiological regulation of thinking: brain-computer interface (BCI) research. Prog. Brain Res. 159, 369–391.

Carelli, R.M., 2002. The nucleus accumbens and reward: neurophysiological investigations in behaving animals. Behav. Cogn. Neurosci. Rev. 1, 281–296.

Caria, A., Veit, R., Sitaram, R., Lotze, M., Weiskopf, N., Grodd, W., Birbaumer, N., 2007. Regulation of anterior insular cortex activity using real-time fMRI. NeuroImage 35, 1238–1246.

Cavanna, A.E., Trimble, M.R., 2006. The precuneus: a review of its functional anatomy and behavioural correlates. Brain 129, 564–583.

Cojan, Y., Waber, L, Schwartz, S., Rossier, L., Forster, A., Vuilleumier, P., 2009. The brain under self-control: modulation of inhibitory and monitoring cortical networks during hypnotic paralysis. Neuron 62, 862–875.

Day, J, Carelli, R., 2007. The nucleus accumbens and Pavlovian reward learning. Neuroscientist 13, 148–159.

deCharms, R., 2007. Reading and controlling human brain activation using real-time functional magnetic resonance imaging. Trends Cogn. Sci. 11, 473–481.

deCharms, R., Christoff, K., Glover, G., Pauly, J., Whitfield, S., Gabrieli, J., 2004. Learned regulation of spatially localized brain activation using real-time fMRI. NeuroImage 21, 436–443.

deCharms, R.C., Maeda, F., Glover, G.H., Ludlow, D., Pauly, J.M., Soneji, D., Gabrieli, J.D., Mackey, S.C., 2005. Control over brain activation and pain learned by using real-time functional MRI. Proc. Natl. Acad. Sci. U. S. A. 102, 18626–18631.

Harrison, B.J., Pujol, J., Ortiz, H., Fornito, A., Pantelis, C., Yücel, M., 2008. Modulation of brain resting-state networks by sad mood induction. PLoS One 3, e1794.

Lang, P.J., Bradley, M.M., Cuthbert, B.N., 1999. International Affective Picture System (IAPS): Technical Manual and Affective Ratings. University of Florida, Center for Research in Psychophysiology, Gainesville, FL.

Linden, D.E., 2006. How psychotherapy changes the brain—the contribution of functional neuroimaging. Mol. Psychiatry 11, 528–538.

Lorr, M., McNair, D.M., Droppleman, L.F., 1971. POMS™ Profile of Mood States. Multi-Health Systems Inc., North Tonawanda, NY.

Phan, K.L., Wager, T., Taylor, S.F., Liberzon, I., 2002. Functional neuroanatomy of emotion: a meta-analysis of emotion activation studies in PET and fMRI. NeuroImage 16, 331–348.

Posse, S., Fitzgerald, D., Gao, K., Habel, U., Rosenberg, D., Moore, G.J., Schneider, F., 2003. Real-time fMRI of temporolimbic regions detects amygdala activation during single-trial self-induced sadness. NeuroImage 18, 760–768.

Rota, G., Sitaram, R., Veit, R., Erb, M., Weiskopf, N., Dogil, G., Birbaumer, N., 2009. Self-regulation of regional cortical activity using real-time fMRI: the right inferior frontal gyrus and linguistic processing. Hum. Brain Mapp. 30, 1605–1614.

Roseman, I.J., Spindel, M.S., Jose, P.E., 1990. Appraisals of emotion-eliciting events: testing a theory of discrete emotions. J. Pers. Soc. Psychol. 99, 899–915.

Summerfield, J.J., Hassabis, D., Maguire, E.A., 2009. Cortical midline involvement in autobiographical memory. NeuroImage 44, 1188–1200.

Talmi, D., Seymour, B., Dayan, P., Dolan, R.J., 2008. Human Pavlovian-instrumental transfer. J. Neurosci. 28, 360–368.

Van Dillen, L.F., Heslenfeld, D.J., Koole, S.J., 2009. Tuning down the emotional brain: an fMRI study of the effects of cognitive load on the processing of affective images. NeuroImage 45, 1212–1219.

Watson, D., Clark, L.A., Tellegen, A., 1988. Development and validation of brief measures of positive and negative affect: the PANAS scale. J. Pers. Soc. Psychol. 54, 1063–1070.

Weiskopf, N., Veit, R., Erb, M., Mathiak, K., Grodd, W., Goebel, R., Birbaumer, N., 2003. Physiological self-regulation of regional brain activity using real-time functional magnetic resonance imaging (fMRI): methodology and exemplary data. NeuroImage 19, 577–586.

Weiskopf, N, Mathiak, K., Bock, S., Scharnowski, F., Veit, R., Grodd, W., Goebel, R., Birbaumer, N., 2004a. Principles of a brain-computer interface (BCI) based on real-time functional magnetic resonance imaging (fMRI). IEEE Trans. Biomed. Eng. 51, 966–970.

Weiskopf, N., Scharnowski, F., Veit, R., Goebel, R., Birbaumer, N., Mathiak, K., 2004b. Self-regulation of local brain activity using real-time functional magnetic resonance imaging (fMRI). J. Physiol. Paris 98, 357–373.

Yoo, S., O'Leary, H., Fairneny, T., Chen, N., Panych, L., Park, H., Jolesz, F., 2006. Increasing cortical activity in auditory areas through neurofeedback functional magnetic resonance imaging. NeuroReport 17, 1273–1278.